Far-Field RCS Prediction from Measured Near-Field Data Over Ground Plane

Yoshio Inasawa*, Shinji Kuroda, Shinichi Morita, Hitoshi Nishikawa,
Yoshihiko Konishi, Yonehiko Sunahara and Shigeru Makino
Mitsubishi Electric Corporation
5-1-1 Ofuna, Kamakura, Kanagawa 247-8501, Japan
E-mail:inasawa@isl.melco.co.jp

1.Introduction

The far-field Radar Cross Section (RCS) measurement of the actual target requires a long measurement range, which can be realized in the outdoor site. One of the problems in outdoor measurement is the difficulty to avoid the effect of ground bounce. Some sites realize the outdoor RCS measurement in a few kilometer range by the exploitation of the ground bounce [1][2]. The shorter measurement range would be preferable. In this paper we present the results of far-field RCS prediction from near-field data over the ground plane in order to investigate the measurement range reduction. We adopt near-field to far-field transformation techniques [3][4]. Some models are measured over the metal ground inside an indoor anechoic chamber. We evaluate the validity of the near-field RCS measurement over ground plane.

2. Near-Field RCS Measurement Including Ground Bounce

Figure 1 shows RCS measurement over the ground plane. The radiowave emitted from transmit antenna is reflected by the target and returned to receive antenna via four multi-paths according to the ground bounce. The RCS measurements over ground plane are achieved on the condition that the scattered fields by four multi-paths are considered to be identical. This condition is described as follows

$$HaHt=nR\lambda/4 \text{ (n is odd number).} \quad (1)$$

The condition of n=1 is usually adopted. The received power is increased by 12dB because of the synthesis of the scattered fields.

Sometimes, it is difficult to achieve the RCS measurement of actual target in the far-field region. The near-field to far-field RCS transformation techniques[3][4] are often adopted in such cases. The algorithm of the transformation is based on the imaging techniques. The scattering coefficient: $S_e(y)$ of a target is obtained from the near-field electric field:$E_s(\phi)$ as follows:

$$S_e(y) = 2jR^2 \exp\left(jk(2R + y^2/R)\right)\int_{\phi w} E_s(\phi)\exp(-2jk\phi y)d\phi \,. \quad (2)$$

The far-field RCS is easily obtained by integrating the obtained scattering coefficient.

3. Measurement and Simulation Results

We present the simulation results of the far-field RCS prediction from near-field data including the ground bounce. The near-field data is measured on the metal ground plane in an anechoic chamber, not on the actual ground plane, as shown in Fig.2 and Fig.3 because the fundamental characteristics of ground bounce would become evident. The V-pol. reflection coefficient of metal is opposite to that of actual ground in case of grazing incidence. The required condition for the V-pol. measurement

ISBN: 89-86522-78-0 94460©KEES

becomes to be n=2 in (1).

First we show the predicted result of Model 1 from one dimensional near-field data. The specifications of measurement are shown in Table 1. The measurement range: R=12m is 50% of the standard far-field condition ($= 2D^2 / \lambda$) regarding the horizontal dimension of the target. Meanwhile, the far-field condition regarding the vertical dimension of the target is satisfied. The predicted results for HH-pol. and VV-pol. are shown in Fig.4 (a) and Fig.4 (b), respectively. Also presented is the computed far-field RCS by equivalent edge current method. It is shown that the predicted far-field RCS for HH-pol. agrees well with computed one. However the predicted result for VV-pol. has small error. The larger difference of multi-path's scattering angle for VV-pol. causes the error. Next we show the predicted far-field RCS of Model 2 that has the dimensions of 0.6m(Y) and 0.6m(Z). The measurement range: R=12m is 50% of the far-field condition regarding both the horizontal and vertical dimensions. Thus the far-field RCS will be predicted from two dimensional near-field data. Fig.5 shows the predicted far-field RCS. It is shown that two dimensional near-field data is necessary for the far-field RCS prediction. However there exists small error. The cause of the error is that the measurement condition of (1) is not satisfied by the large vertical dimension of the measurement model. The error is inherent in the RCS measurement over ground plane.

Finally, we show the far-field RCS prediction for Model 1 with another scattering object shown in Fig.6(a). Near-field and far-field RCS are computed by equivalent edge current method. The far-field RCS is predicted using scattering coefficient data of (2) inside the region correspond to the dimension of model 1. The predicted far-field RCS is shown in Fig.6(b). It is shown that the distortion of RCS pattern is removed in the predicted far-field RCS. This effect is an advantage of near-field RCS measurement.

4. Conclusions

We presented the predicted far-field RCS from measured and computed near-field RCS over the metal ground. It was shown that the near-field RCS measurement techniques could predict far-field RCS. However the inherent error of the RCS measurement over the ground plane existed for the measurement model with large vertical dimension.

References

[1]Nucholas C.Currie, Ed., "Techniques of Radar Reflectivity Measurement", Artech House, 1984.

[2]Rodger D. Nichols, et al., "Ansi Z-540/ISO 25 Certification Activities at the Lockheed Martin Helendale Outdoor RCS Range," AMTA2001 ,pp.20-25.

[3]David G. Falconer; "Extrapolation of near-field RCS measurements to the far zone," IEEE Trans. Antennas Propagat, Vol. 36, pp. 822 - 829, June 1988.

[4]Yoshio Inasawa, et al., "Far-Field RCS Prediction Method Using Cylindrical or Planar Near-Field RCS Data," IEICE Trans. Electron. Vol.E80-C, No.11, pp1402-1406, Nov. 1997.

Table 1 Measurement Specifications

Frequency(GHz)	10.0
R(m)	12.0
Ht(m)	0.9
Model 1	600(Y) x 200(Z) x 250(X)
Model 2	600(Y) x 600(Z) x 250(X)

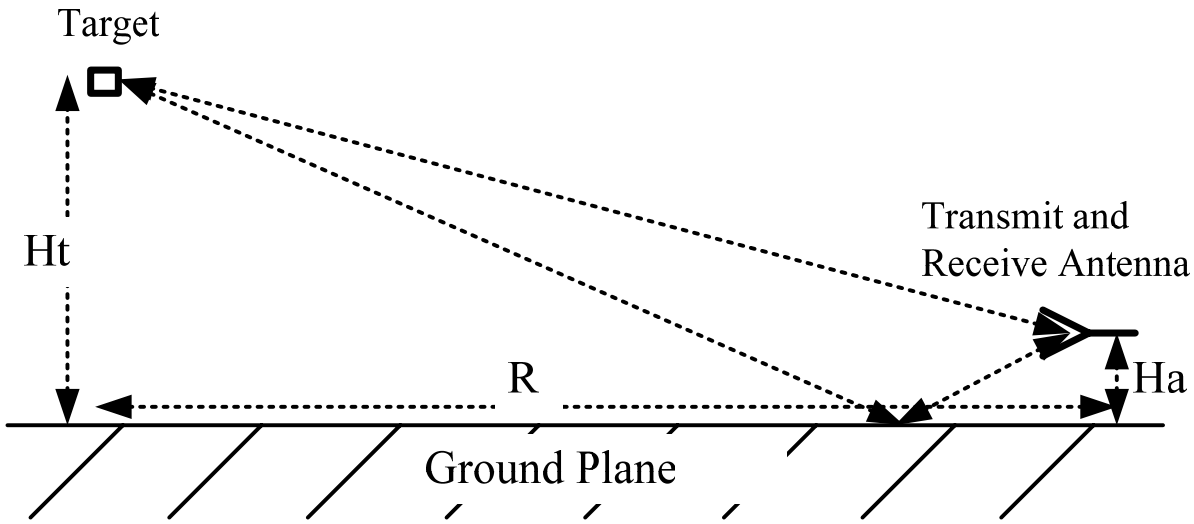

Fig.1 RCS Measurement including Ground Plane Bounce.

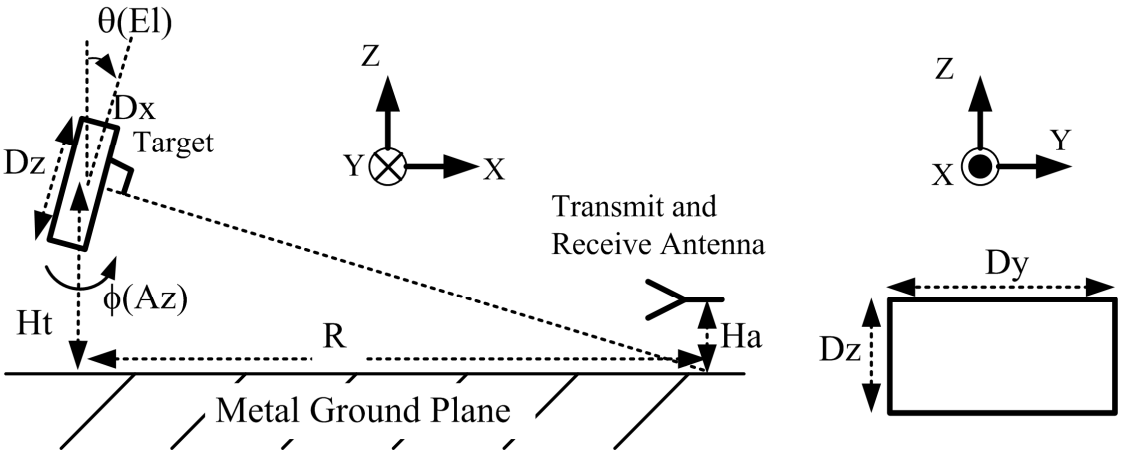

(a) Coordinate System. (b) Model Dimension.

Fig.2 Coordinate System for Near-Field RCS Measurement.

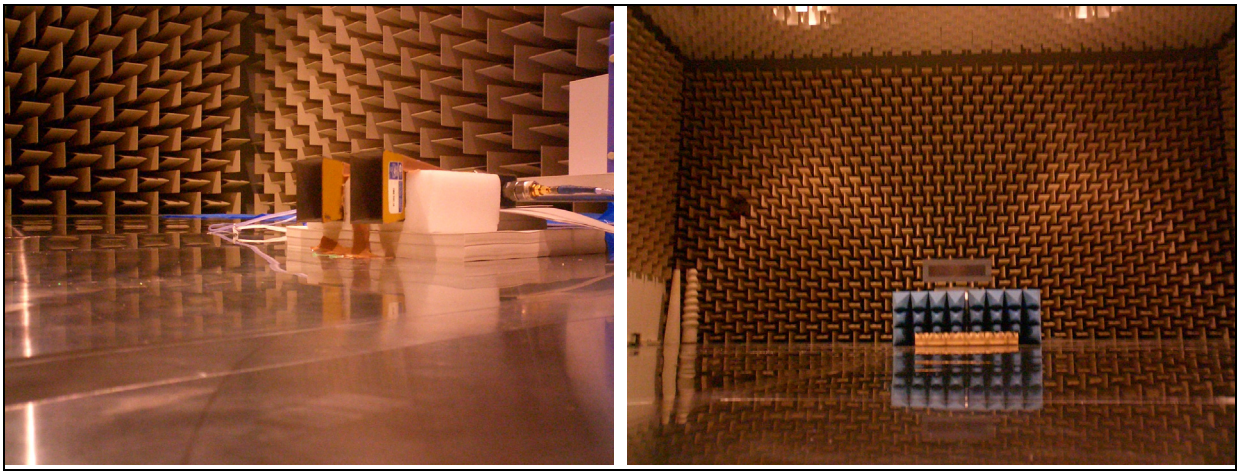

(a) Receive and Transmit Antennas. (b)Measurement Model.

Fig.3 RCS Measurement Appearance.

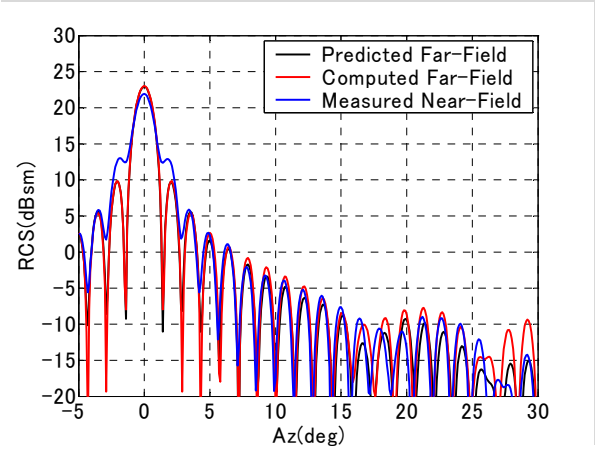

(a)HH-pol.(Ha=0.1m(n=1))

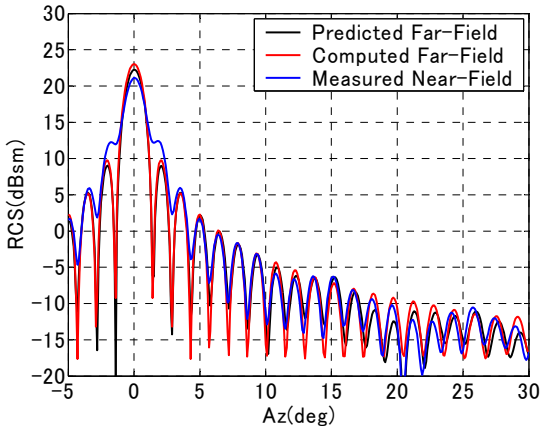

(b)VV-pol.(Ha=0.2m(n=2))

Fig.4 Far-Field RCS Prediction from 1D Near-field data.

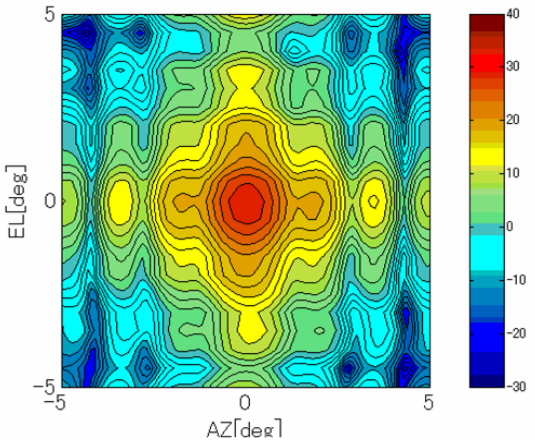

(a)2 Dimensional RCS Pattern.

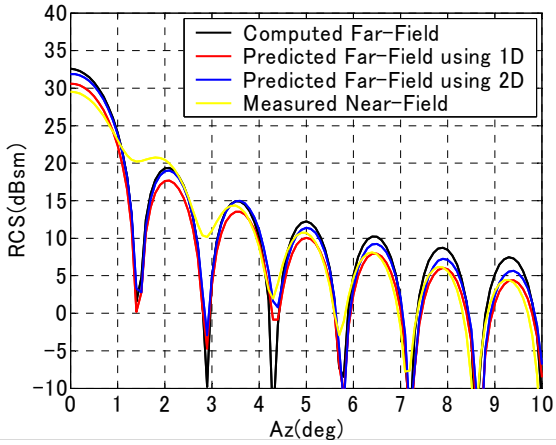

(b)Predicted Result.

Fig.5 Far-Field RCS Prediction from 2D Near-field data.(HH pol., Ha=0.1m)

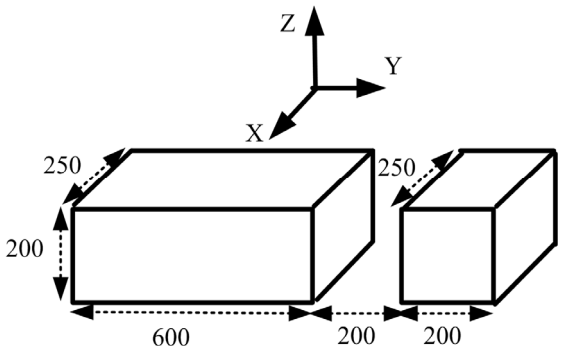

(a)Model 1 with a Scattering Object

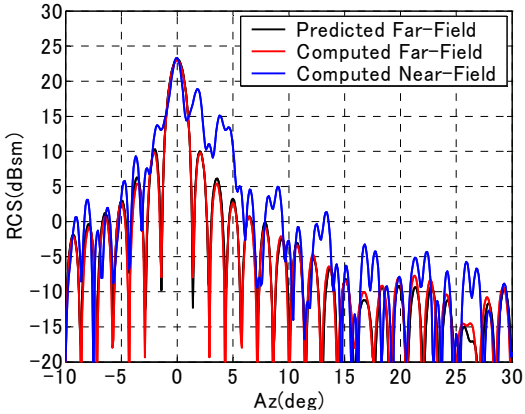

(b)Predicted Result.

Fig.6 Far-Field RCS Prediction from 1D Near-field data with a Scattering Object.